

# Reliability analysis of soil slope reinforced by micro-pile considering spatial variability of soil strength parameters

Yuke Wang<sup>1,2</sup>, Haiwei Shang<sup>1,2</sup>, Yukuai Wan<sup>\*3</sup> and Xiang Yu<sup>1,2</sup>

<sup>1</sup>School of Water Conservancy and Transportation, Zhengzhou University, Zhengzhou, 450001, China

<sup>2</sup>Henan Key Laboratory of Grain and oil storage facility and safety, Henan University of Technology, Zhengzhou, 450001, China

<sup>3</sup>School of Civil and Hydraulic Engineering, Ningxia University, Yinchuan, 750021, China

(Received August 3, 2022, Revised November 29, 2023, Accepted March 18, 2024)

**Abstract.** In the traditional slope stability analysis, ignoring the spatial variability of slope soil will lead to inaccurate analysis. In this paper, the K-L series expansion method is adopted to simulate random field of soil strength parameters. Based on Random Limit Equilibrium Method (RLEM), the influence of variation coefficient and fluctuation range on reliability of soil slope supported by micro-pile is investigated. The results show that the fluctuation ranges and the variation coefficients significantly influence the failure probability of soil slope supported by micro-pile. With the increase of fluctuation range of soil strength parameters, the mean safety factor of the slope increases slightly. The failure probability of the soil slope increases with the increase of fluctuation range when the mean safety factor of the slope is greater than 1. The failure probability of the slope increases by nearly 8.5% when the fluctuation range is increased from  $\delta_v=2$  m to  $\delta_v=8$  m. With the increase of the variation coefficient of soil strength parameters, the mean safety factor of the slope decreases slightly, and the probability of failure of soil slope increases accordingly. The failure probability of the slope increases by nearly 31% when the variation coefficient increases from  $COV_c=0.2$ ,  $COV_\phi=0.05$  to  $COV_c=0.5$ ,  $COV_\phi=0.2$ .

**Keywords:** micro-pile; spatial variability; monte-carlo method; random limit equilibrium method (RLEM); soil slope

## 1. Introduction

Due to the long-term, multi-cycle geological action and the varying intensity and complexity of the geological action, the properties of soils vary greatly in nature (Degroot and Baecher 1993, Phoon and Kulhawy 1999a). In general, soil parameters always have regularity in spatial distribution, and this regularity is mainly controlled by factors such as sedimentation and sedimentary environment (Fenton and Vanmarcke 1991, Phoon and Kulhawy 1999b, Wang *et al.* 2023). Traditional method is to judge the stability state of slope by taking safety factor as evaluation index (Zhang *et al.* 2023). This deterministic analysis method can't consider the spatial variability of soil strength parameters, and slope failure may occur even though the safety factor is high (Huang *et al.* 2019, Pang *et al.* 2021, Wang *et al.* 2022b). In order to explore the influence of spatial variability of soil strength parameters on slope reliability, scholars used random field to describe the spatial variability of soil strength parameters. Considering the uncertainty of soil mass, the failure probability of slope is usually used as an effective index to evaluate the reliability of slope. Monte-Carlo simulation method is widely used in calculating slope failure probability (Cho 2010, Jiang *et al.* 2015, Xu *et al.* 2020, Zhou *et al.* 2003, Pang *et al.* 2023). Many scholars have also studied the influence of

geotechnical spatial variability on slope reliability by random finite difference method (RFDM) (Cheng *et al.* 2018, Li *et al.* 2017), random limit equilibrium method (RLEM) (Cho 2010, Fenton and Griffiths 2003, Griffiths *et al.* 2011, Javankhoshdel *et al.* 2017), and random finite element method (RFEM) (Griffiths and Fenton 2004, Griffiths *et al.* 2009, Luo *et al.* 2016, Suchomel and Masin 2010).

In recent years, anti-slide piles are mainly used to reinforce the slope with an excellent reinforcement effect. As a kind of lateral loaded pile, anti-slide pile can provide lateral anti-sliding force and play anti-sliding role together with soil around the pile. Many scholars have studied the design optimization and reinforcement mechanism of anti-slide pile. Tang *et al.* (2018) studied the influence of pile length, position of pile sheet, pile stiffness and soil properties on the performance of piles. Li *et al.* (2019) and Mao *et al.* (2019) found that the deformation patterns of adjacent piles in pile groups are different, resulting in different degrees of axial forces and bending moments. The above scholars usually take safety factor or numerical analysis results as evaluation indexes, when evaluating the reinforcement effect of anti-slide piles. These methods have proved to be ineffective in considering the uncertainty of actual loads and material parameters. Teixeira *et al.* (2012) analyzed the reliability of the vertically loaded pile. Chen *et al.* (2020) carried out deterministic stability analysis on soil slope reinforced by pile at different locations and lengths, and determined failure probability by random limit equilibrium method (RLEM). Based on Hoek-Brown criterion and RFDM, Zhang *et al.* (2021) carried out

\*Corresponding author, Ph.D.  
E-mail: wanyukuai@163.com

reliability analysis of slope stability and random response of piles considering spatial variability of rock mass. Based on the load transfer method and RFDM, Luo *et al.* (2019) discussed the influence of vertical spatial variability of soil parameters on the ultimate bearing capacity state and the design scheme of normal service limit state of single energy pile. It was found that neglecting spatial variability of soil would overestimate the failure probability of energy pile under two ultimate states. Some scholars consider the influence of space variability of rock and soil mass on engineering stability and pile foundation. Most of the research objects in these achievements are ordinary anti-slide pile types. There are significant differences between micro-pile and traditional anti-sliding pile in reinforcement mechanism, stress mode, optimum design, etc. There is a lack of research on reliability of micro-pile supporting soil slope.

Since Latin hypercube divides sampling units into different layers according to a characteristic or a rule, samples are taken independently and randomly from different layers. This ensures that the structure of the sample is similar to that of the population, thus improving the accuracy of the estimation. In this paper, random fields generated by using K-L series expansion method and Latin Hypercubic sampling method are used to simulate the spatial variability of soil strength parameters. Based on Random Limit Equilibrium Method (RLEM) and Monte-Carlo Simulation (MCS), the influence of variation coefficient and fluctuation range on the reliability of soil slope supported by micro-pile is explored.

## 2. Reliability analysis method of soil slope supported by micro-pile

In this paper, the limit state equation of the two-dimensional soil slope supported by micro-pile is established based on the limit equilibrium method. The random field of internal friction angle and cohesion is generated by K-L series expansion method. Finally, the failure probability of the slope supported by micro-pile is calculated by Monte-Carlo method.

### 2.1 Monte Carlo simulation

During the calculation of slope reliability, the limit state equation is usually defined as  $g(x)=F(x)-1$ . The results of the limit state equation determine whether the slope has the risk of destabilization. When  $g(x)>0$ , the slope is in a stable state; when  $g(x)=0$ , the slope is in a critical state; when  $g(x)<0$ , the slope is in an unstable state. The slope failure probability  $P_f$  can be expressed as Eq. (1) (Wan *et al.* 2023, Wang *et al.* 2022a, 2024).

$$P_f = \int_{g(x) \leq 0} f(x) dx = E_{f(x)} \{I[g(x)]\} \quad (1)$$

$I[g(x)]$  is an indicator function, when  $g(x) \leq 0$ ,  $I[g(x)]$  is set to 1; when  $g(x) > 0$ ,  $I[g(x)]$  is set to 0.  $E_{f(x)}$  is the mathematical expectation operator under the joint probability density function  $f(x)$ .

The estimated value of slope failure probability  $P_f$  calculated by the MCS method can be expressed as Eq. (2) (Wan *et al.* 2023, Wang *et al.* 2022a, 2024).

$$\hat{P}_f = \frac{1}{N} \sum_{i=1}^N I[g(x_i)] = \frac{n_s}{N} \quad (2)$$

In the Eq. (2):  $x_i$  ( $i=1, 2, 3, \dots, N$ ) is the random sample simulated by the parameter joint probability density function  $f(x)$ .  $n_s$  is the number of failed samples.

### 2.2 Random field model representing spatial variability of soil parameters

The random field model can effectively represent the spatial variability of soil parameters. The correlation between soil parameters at different points in space is described by the auto-correlation function. In this paper, two-dimensional exponential auto-correlation function is used to describe the spatial variability of soil parameters, the expressions can be expressed as Eq. (3) (Cho 2010).

$$\rho(x, y) = \exp\left(-\frac{|x-x'|}{l_h} - \frac{|y-y'|}{l_v}\right) \quad (3)$$

In Eq. (3),  $l_v$  and  $l_h$  represent the vertical and horizontal auto-correlation distances respectively. The fluctuation range refers to that within a certain space of soil, and the correlation between properties parameters gradually decreases with the increase of the distance between two points. The fluctuation range can be neglected when the distance is greater than a certain value.  $\delta_v$  and  $\delta_h$  represent the fluctuation ranges in horizontal and vertical directions respectively. In two-dimensional exponential auto-correlation functions,  $\delta_{v(h)}=2l_{v(h)}$ .  $(x, y)$ ,  $(x', y')$  represent the coordinates of any two points in space.

The random fields of parameters need to be discretized into random variables to carry out reliability analysis. In this paper, the K-L series expansion method is used to discrete random parameters into a set of 2-D lognormal random field, the K-L series decomposition is shown in Eq. (4) (Cho 2010).

$$H(x, y) = \exp\left[\mu + \sum_{i=1}^n \sigma \sqrt{\lambda_i} f_i(x, y) \varepsilon_i\right], x \in \Omega \quad (4)$$

In Eq. (4),  $\Omega$  is the spatial set.  $H(x, y)$  is the random field of some soil parameters.  $(x, y)$  is the physical space coordinate of the random field.  $\mu$  and  $\sigma$  represent the mean and standard deviation of random parameters respectively.  $\varepsilon_i$  is an independent standard normal random variable,  $\lambda_i$  and  $f_i(x, y)$  represent the eigenvalues and eigenfunctions corresponding to the directional correlation function respectively.  $n$  is the number of truncated items.

## 3. Limit state equation of micro-pile supporting slope based on limit equilibrium method

### 3.1 Anti-sliding force of slope supported by micro-pile

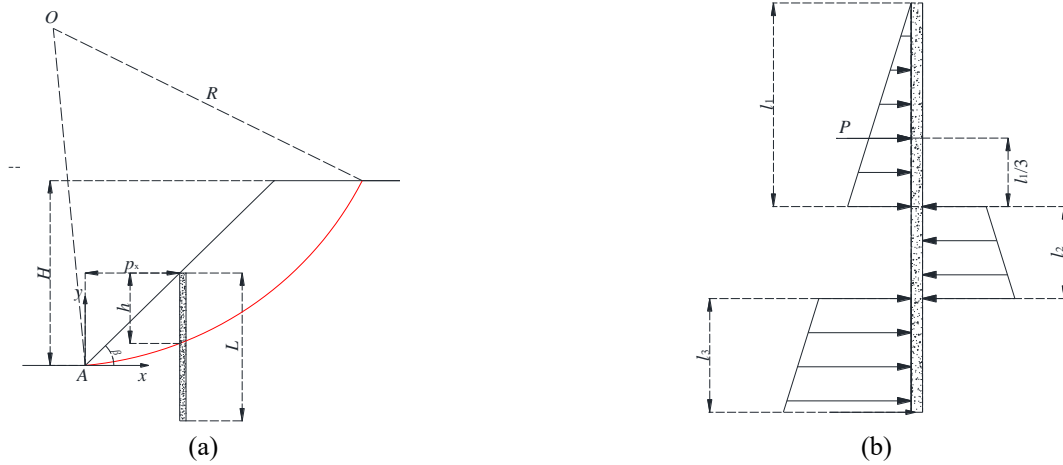


Fig. 1 Internal force distribution of slope supported by micro-pile

In this paper, the mechanical analysis model of micro-piles is consistent with that of Deng *et al.* (2017). Fig. 1. shows the internal force analysis diagram of micro-pile supporting slope. Establishing two-dimensional coordinate system with point A as the center of circle, horizontal direction as the  $x$ -axis, vertical direction for the  $y$ -axis. The height of the slope is  $H$  and the length of the pile is  $L$ . The horizontal position between pile position and slope foot is  $p_x$ . The slope angle is  $\beta$ . Assuming that the sliding surface is circular arc, the coordinates of the center of the sliding surface are  $(x_0, y_0)$ , the radius is  $R_0$ , and the length of the pile above the sliding surface is  $h$ .

Due to the influence of external force, only part of the anti-sliding force provided by the micro-pile can play a role, the effective side force of micro-pile the acts on sliding mass only in the limited state of the slope. Therefore, in the calculation process, the slope is assumed to be in the limit equilibrium state. Meanwhile, taking into account that the actual spatial arrangement of the micro-piles is inconsistent with this assumption, the effective micro-pile side force ( $P$ ) can be amended using the coefficient  $D/S_p$ , where  $D$  = diameter of the micro-pile, and  $S_p$  = horizontal spacing of the micro-piles in the longitudinal section of the sliding body. In this study, the coefficient  $D/S_p$  was set to 1.

The anti-sliding force provided by micro-pile is related to its self-strength and embedded depth. In this paper, it is assumed that the micro-pile has sufficient strength and won't be damaged in the process of reinforcement. Therefore, the embedding depth of the micro-pile is the main factor affecting the reinforcement effect of micro-pile. During the process of micro-pile supporting soil slope, the pile body is mainly divided into three parts (Deng *et al.* 2017): (1) The part above the sliding surface: this part is mainly determined by the length of the pile on the sliding surface; (2) pressure generated by the soil behind the pile; (3) The lower part of the sliding surface is determined by the earth pressure in front of the pile. Assuming that the earth pressure is triangular distribution, with its coefficient  $k_0$ , and it is equal to zero on the slope surface. The coefficient  $k_0$  can be obtained by in situ testing, or it can be estimated using  $(k_p - k_a)$ , where  $k_p$  is the passive earth pressure coefficient, and  $k_a$  is the active earth pressure

coefficient. In addition, for the convenience of calculation, the effective lateral pressure of micro-pile is simplified as triangular distribution pressure, which acts on  $2/3$  of the pile length on the sliding surface, where  $\lambda$  = scale coefficient,  $h$  = height is in the sliding body.

The static equilibrium equation of pile in the horizontal direction is shown in Eq. (5).

$$\frac{1}{2} \lambda k_0 \gamma_1^2 + \frac{1}{2} k_0 \gamma [(l - l_3) + l] \gamma_3 = \frac{1}{2} k_0 \gamma [(l - l_3) + l] [(l - l_3) - l_1] \quad (5)$$

From Eq. (6), it can be concluded that the scaling coefficient is Eq. (6).

$$\lambda = \frac{2(l - l_3)^2 - l^2 - l_1^2}{l_1^2} \quad (6)$$

The torque equilibrium equation of pile force at point e is shown in Eq. (7).

$$\frac{1}{6} \lambda k_0 \gamma_1^3 + \frac{1}{6} k_0 \gamma [2(l - l_3) + l] [(l - l_3) - l_1]^2 = \frac{1}{6} k_0 \gamma \{3(l - l_1) [(l - l_3) + l] \gamma_3 - [2(l - l_3) + l] \gamma_3^2\} \quad (7)$$

According to Eqs. (5)-(7), the proportional coefficient  $\lambda$  can be obtained, and then the anti-sliding force  $P$  provided by a single anti-sliding pile can be obtained through Eq. (8) (Deng *et al.* 2017).

$$P = \frac{1}{2} \lambda k_0 \gamma_1^2 \quad (8)$$

### 3.2 Limit state equation of soil sope supported by micro-pile

The Simplified Bishop method assumes that the slip surface is circular arc. In this paper, to make the results more reasonable, the range of the slide-out and slide-in are divided into  $n_1$  and  $n_2$  parts, and the range of the tangent divided into  $n_3$  parts,  $n_1 \times n_2 \times n_3$  circular sliding surfaces are generated finally. By calculating the safety factor of each circular sliding surface, the minimum safety factor and its corresponding sliding surface are searched. The force of soil strip and pile as shown in the Fig. 2. For the Simplified Bishop method, the formulas of the slope FOS ( $F_s$ ), normal force ( $N_j$ ) on the slip surface, and shear force ( $T_j$ ) on the slip

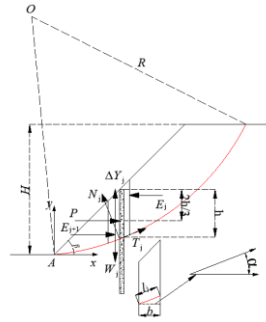


Fig. 2 Force distribution of soil strip and micro-pile

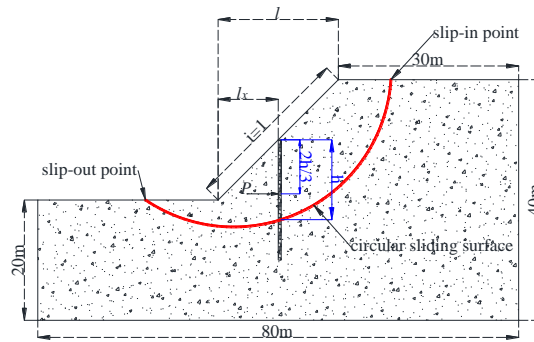


Fig. 3 Calculation model

surface are given as Eqs. (10)-(13).  $m$  is the number of soil strips.  $W_j$  is the gravity of the soil strip.  $Y_j$  is the shearing force between soil strips.  $l_j$  is the arc length of the soil strip.  $\alpha_j$  is the angle between the tangent of the arc and the positive direction of the  $x$ -axis. The specified positive direction is the counterclockwise rotation direction of the  $x$ -axis.

$$N_j = \frac{1}{m_{aj}} \left( W_j + \Delta Y_j - \frac{cl_j \sin \alpha_j}{F_s} \right) \quad (9)$$

$$T_j = \frac{1}{F_s m_{aj}} \left[ (W_j + \Delta Y_j) \tan \varphi + cl_j \cos \alpha_j \right] \quad (10)$$

$$m_{aj} = \cos \alpha_j + \frac{\tan \varphi \sin \alpha_j}{F_s} \quad (11)$$

The inter-slice forces between soil strips is internal force which isn't reflected in the equilibrium equation and assumes that  $Y_j$  is 0. The moment equilibrium equation is established for the whole. The solution is obtained by using the moment equilibrium condition, shown in Eq. (12),  $g$  is the number of micro-pile.

$$\sum_{j=1}^m W_j R \sin \alpha_j - \sum_{j=1}^m T_j R - \sum_{k=1}^g P_k \left( R \cos \alpha_k - \frac{1}{3} h \right) = 0 \quad (12)$$

Solving the safety factor by iteration, as

$$F_s = \frac{\sum_{j=1}^m \frac{1}{m_{aj}} [W_j \tan \varphi + cb]}{\sum_{j=1}^m [W_j \sin \alpha_j] - \sum_{k=1}^g P_k \left( \cos \alpha_k - \frac{1}{3} \frac{h}{R} \right)} \quad (13)$$

#### 4. Numerical calculation and working condition of micro-pile supporting soil slope

##### 4.1 Introduction to numerical model

The calculation model is 80 m in length and 40 m in height. The slope height is 20 m, and the slope angle of the model is 45°. The size of the random field is 40 m\*80 m, as shown in Fig. 3. The strength parameters of soil follow the lognormal distribution, the mean value of cohesion  $c=12$  kPa, the mean value of internal friction angle  $\varphi=26^\circ$ .

Compared with other engineering materials, the parameters of geotechnical materials show great uncertainty. In recent decades, scholars have conducted many studies on the variability of geotechnical parameters. Mayer and Stead (2017) found that the correlation length of spatial variation ranged from tens to hundreds of meters. Fenton and Vanmarcke (1991) believes that the fluctuation range of soil parameters mainly depends on the geological process of soil deposition, rather than the specific soil properties. The spatial variation characteristics of soil mass can be roughly judged based on the empirical judgment of geological causes. There are obvious differences in soil strength parameters at different spatial locations, when the fluctuation range and variation coefficient of soil strength parameters change, as shown in Fig. 4. Table 1 shows the fluctuation range values of different soils reported by different scholars (Asaoka and Agrivas 1982, Chiasson *et al.* 1995, Soulie *et al.* 1990). These statistics show that the fluctuation range of soil in the vertical direction is generally between 0.2 and 8 m, and that in the horizontal direction is generally between 20 m and 80 m. Duncan *et al.* (2000,

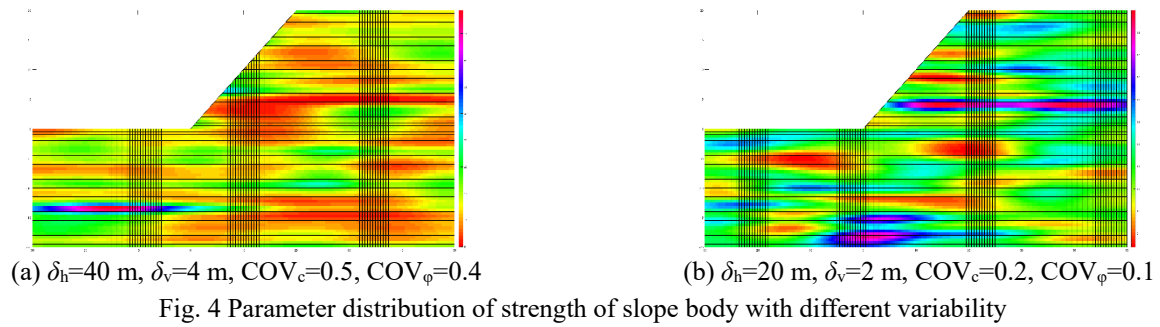


Table 1 Statistical data of fluctuation range of different soil strength parameters (Asaoka and Agrivas 1982, Chiasson *et al.* 1995, Soulie *et al.* 1990)

Parameter	The soil type	Fluctuation range	
		Vertical	Horizontal
Su	Sensitive clay (Soulie <i>et al.</i> 1990)	8	60
Su	Organic soft clay (Asaoka and Agrivas 1982)	2.4	—
Su	Very soft clay (Asaoka and Agrivas 1982)	2.2	44.2
Su (Qu)	Soft clay (Chiasson <i>et al.</i> 1995)	4	80
Qc	Silty clay (Chiasson <i>et al.</i> 1995)	0.2	20

Table 2 Value range of variation coefficient of main geotechnical parameters (Duncan 2000, Phoon 2008)

The soil parameters	Typical coefficient of variation	Recommended coefficient of variation (when data is insufficient)
Bulk density ( $\gamma$ ) (Duncan 2000)	0.01~0.1	0
Cohesion ( $c$ ) (Duncan 2000)	0.19~0.55	0.3
Angle of internal friction ( $\phi$ ) (Duncan 2000)	0.05~0.4	0.2
Undrained shear strength ( $C_u$ ) (Phoon 2008)	0.2~0.4	0.2

Table 3 Variation coefficients of soil strength parameters

Group	COV	
	Cohesion ( $c$ )	Internal friction angle ( $\phi$ )
A	0.5	0.05
B	0.4	0.05
C	0.3	0.05
D	0.2	0.05
E	0.2	0.1
F	0.2	0.15
G	0.2	0.2

2008) summarized the value range of variation coefficient of some geotechnical parameters obtained by different test methods and different regions. Table 2 summarizes the value range of variation coefficient of several main geotechnical parameters affecting slope stability.

In this paper, cohesion  $c$  and internal friction angle  $\phi$  are regarded as random field variables, both of which obey lognormal distribution. In this paper, two cases are selected to explore the influence of fluctuation range on the reliability of soil slope supported by micro-piles. (1)  $\delta_v=8$  m,  $\delta_h=20, 30, 40, 50, 60$  m, (2)  $\delta_h=40$  m,  $\delta_v=2, 4, 6, 8$  m. At the same time, the influence of seven groups of variation coefficient on the reliability of micro-pile slope was investigated. The variation coefficient of the first four groups kept  $COV_\phi$  unchanged and  $COV_c$  decreased. The

latter four groups of data enable  $COV_\phi$  increased. The influence of variation coefficient of single strength parameter on the reliability of the slope was investigated. Values of the variation coefficient of the seven groups are shown in Table 3.

#### 4.2 Failure probability calculation process of micro-pile supporting slope

The basic steps of the calculation process of slope reliability of micro-pile support based on limit equilibrium method are as follows:

- (1) Statistical characteristics of input parameters (mean value, standard deviation, distribution type and correlation coefficient of cohesion and internal friction angle; auto-correlation function and fluctuation range of soil spatial variability);
- (2) Solve the eigenvalue and eigenvector of auto-correlation function;
- (3) The random sample matrix is constructed by generating independent standard normal distribution points based on the Latin hypercube sampling technique;
- (4) The K-L series expansion method is used to discretely generate the non-Gaussian random field of cohesion and internal friction angle;
- (5) The limit state equation of micro-pile slope is established based on the limit equilibrium method;

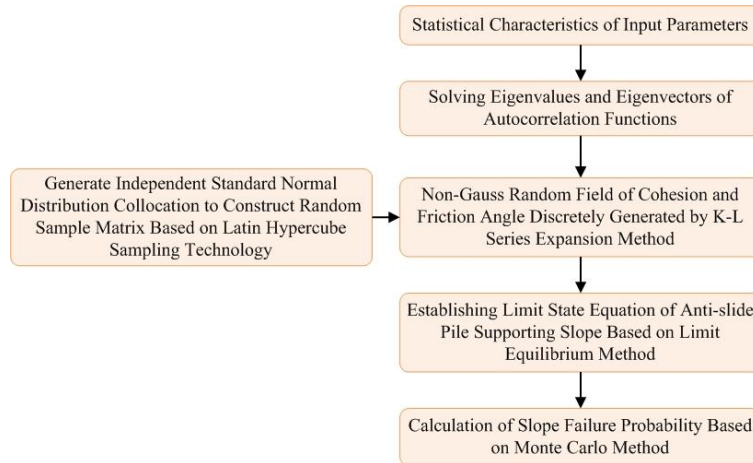


Fig. 5 Reliability calculation process of micro-pile supporting soil slope

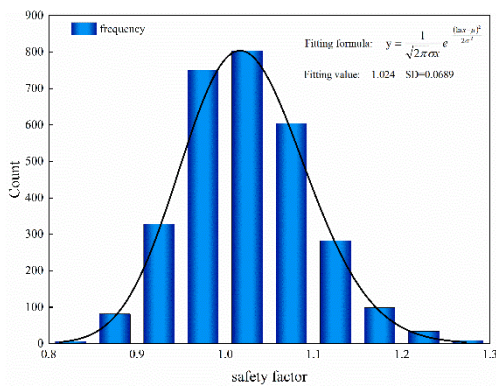


Fig. 6 Normal distribution fitting of safety factor

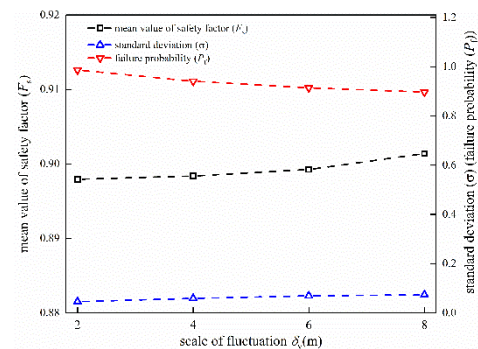


Fig. 7 Evaluation indexes of slope instability under different fluctuation ranges (Without Piles)

(6) Calculate slope failure probability based on Monte-Carlo method.

The calculation process of slope reliability for micro-pile support is shown in Fig. 5.

### 5. Influence on reliability of micro-pile supporting slope

In this section, the influence of soil spatial variation parameters (fluctuation range  $\delta_{v,h}$ , variation coefficient COV) on slope failure probability and the mean safety factor under different design schemes are discussed. It is generally believed that the simulation results are stable and reliable when the variation coefficient of the failure probability  $COV_{Pf} < 0.3$  (Liu *et al.* 2020). In order to improve the computation efficiency and guarantee the accuracy of failure probability, this paper selects the number of Monte-Carlo simulations for 3000 times. The calculation shows that  $COV_{Pf} < 0.3$  meets the requirement of calculation accuracy. The Eq. (14) is used to fit the distribution of soil slope safety factor. The result is shown in Fig. 6, the mean fitting value is 1.024, and the standard deviation(SD) of the fitting is 0.0689.

$$y = \frac{1}{\sqrt{2\pi}\sigma x} e^{-\frac{(\ln x - \mu)^2}{2\sigma^2}} \quad (14)$$

#### 5.1 Influence of fluctuation range on structural reliability

In order to study the influence of fluctuation range on the reliability of slope supported by micro-pile, this paper selects nine working conditions with fluctuation range (1)  $COV_\phi=0.2, COV_c=0.3, \delta_v=8\text{ m}, \delta_h=20, 30, 40, 50, 60\text{ m}$ , (2)  $COV_\phi=0.2, COV_c=0.3, \delta_h=40\text{ m}, \delta_v=2, 4, 6, 8\text{ m}$  respectively to analyze the reliability of slope supported by micro-pile. Under the condition of no piles and  $COV_\phi=0.2, COV_c=0.3$ , the failure probability and safety factor of the slope in different fluctuation ranges are shown in Fig. 7. Fig. 7 shows the mean value of safety factor of slope is less than 1 and increases slightly with the increase of fluctuation range; The probability of slope failure is higher than 90% and tends to decrease with the increase of fluctuation range. With the increase of fluctuation range, the slope safety factor corresponding to 3000 random fields will be more dispersed and the standard deviation of safety factor will increase. Fig. 8 describes the changes of the failure probability of the slope and the standard deviation of the slope safety factor in different fluctuation ranges when the pile position is  $l_x/l=0.5$  and the pile length is 12.5 m. With the increase of the fluctuation range, the failure probability of the slope and the standard deviation of the slope safety factor increase. The reason is that the spatial correlation of soil strength parameters increases and the variability decreases.

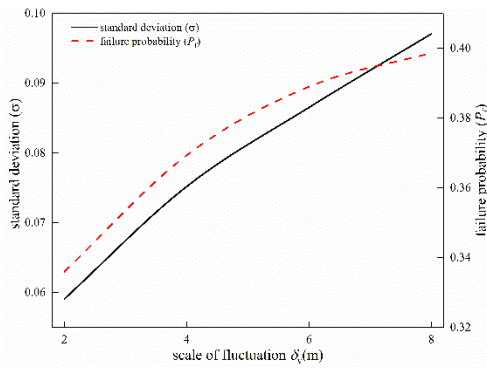


Fig. 8 Failure probability and standard deviation at different fluctuation ranges

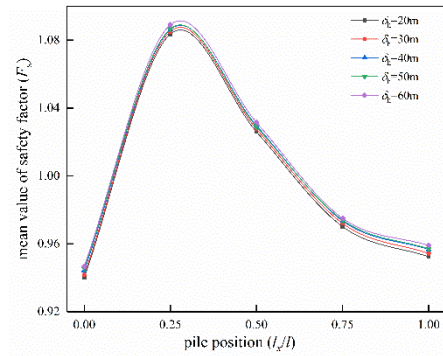


Fig. 11 Safety factors under different pile positions ( $\delta_v=8$  m)

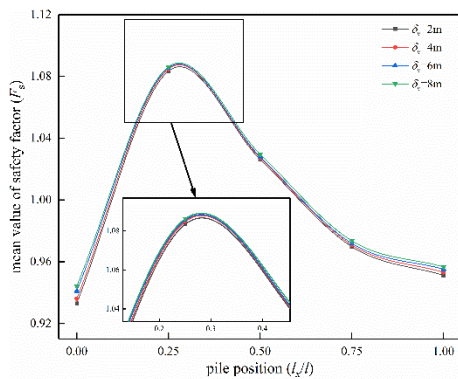


Fig. 9 Safety factors under different pile positions ( $\delta_h=40$  m)

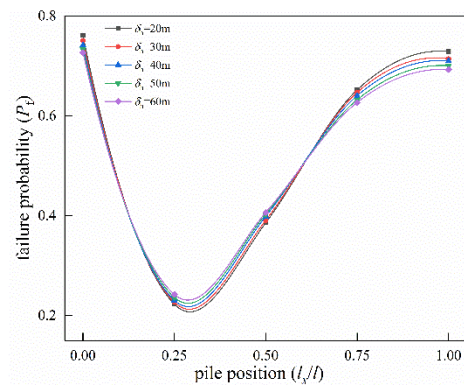


Fig. 12 Failure probability under different pile positions ( $\delta_v=8$  m)

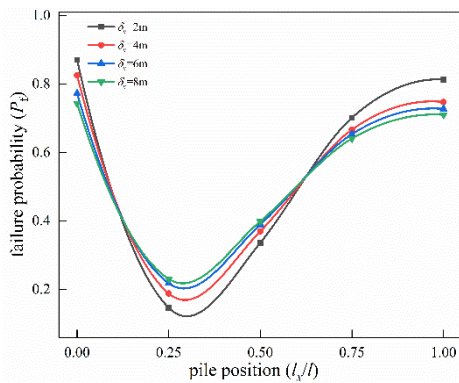


Fig. 10 Failure probability under different pile positions ( $\delta_h=40$  m)

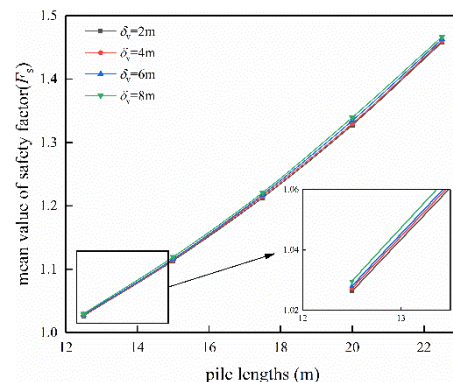


Fig. 13 Safety factors under different pile lengths ( $\delta_h=40$  m)

Figs. 9 and 11 describe the change of the mean value of the slope safety factor when the pile length is 12.5 m and the pile location is different. Figs. 10 and 12 describe the change of the failure probability of the slope. As can be seen from the figure, changes in the fluctuations range have a smaller effect on the safety factor and a larger effect on the failure probability. As shown in Figs. 9 and 11, the mean value of the safety factor of the slope is relatively large when micro-piles are arranged in the lower and middle part of the slope. With the increase of fluctuation range, the safety factor of slope increases. The main reason for this is that when the fluctuations range is small, the strength parameter is more variable and its relevance is smaller. The ability of random field data for soil strength

parameters to provide adequate sliding resistance is related to the fluctuation range in the 3000 Monte-Carlo simulations. As shown in Fig. 8, the standard deviation of the safety factor is positively correlated with the fluctuation range. As a result, when the safety factor is more than 1, the average factor of safety of the slope gradually increases and the probability of failure gradually decreases with the fluctuation range increases.

Although the average safety factor of the slope is greater than 1 when pile is placed in multiple locations, the slope is assessed to be in a safe state from the perspective of safety factor, but slope instability damage probably occurred. At  $l_x/l=0.25$ , the corresponding failure probabilities of  $\delta_v=2$  m and  $\delta_v=8$  m differ by about 8.5%. The corresponding failure

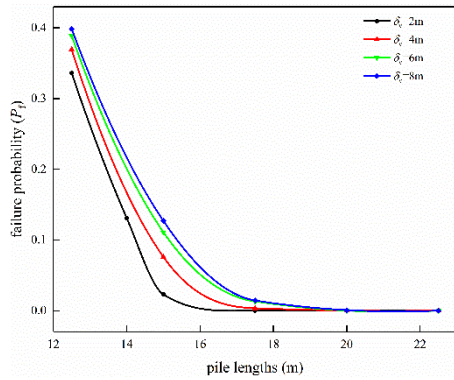


Fig. 14 Failure probability under different pile lengths ( $\delta_h=40$  m)

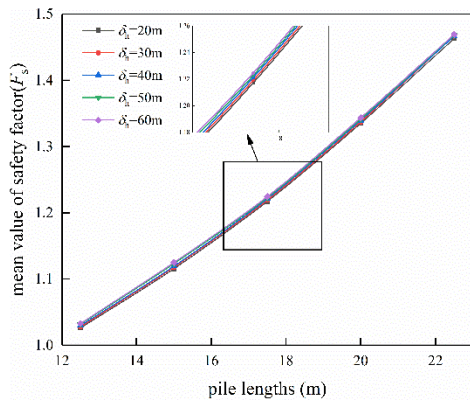


Fig. 15 Safety factors under different pile lengths ( $\delta_v=8$  m)

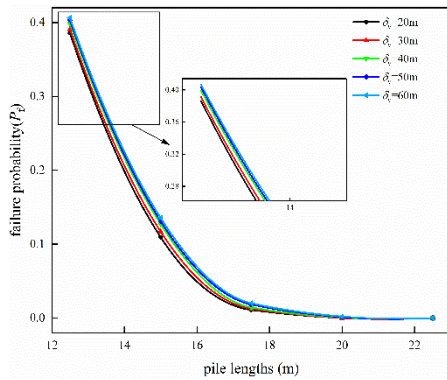


Fig. 16 Failure probability under different pile lengths ( $\delta_v=8$  m)

probabilities of  $\delta_h=20$  m and  $\delta_h=60$  m differ by about 2%. Therefore, the influence of the soil fluctuation range on the failure probability of the slope should be considered in the design of micro-pile. The micro-pile in the lower and middle part of the slope can have the maximum safety factor and the minimum probability of instability.

Figs. 13 and 15 describe the changes of the mean value of the slope safety factor when the pile position is  $l_x/l=0.5$  and the pile length is different. Figs. 14 and 16 describe the changes of the failure probability of the slope. As shown in Figs. 13 and 15, the slope safety factor increases with the increase of pile length. The influence of the fluctuation range on the slope safety factor under different pile lengths

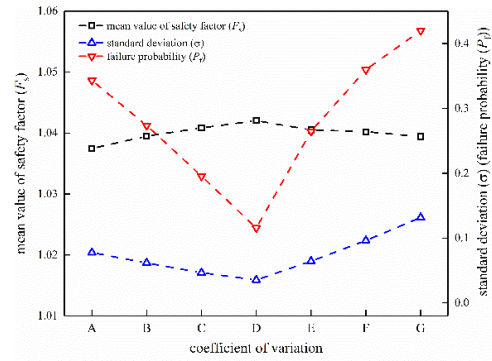


Fig. 17 Evaluation indexes of slope instability under different variation coefficients

shows the same regulation as Fig. 9. As the fluctuation range increases, the mean value of the safety factor is in an upward trend. As shown in Figs. 14 and 16, with the increasing pile length, the failure probability of the slope decreases continuously. The fluctuation range is positively correlated with the failure probability of the slope when the pile length isn't enough. The failure probability of the slope is reduced to 0% when the pile length is long enough.

In the case of  $\delta_v=2$  m, the failure probability of the slope decreases to about 0% when the pile length reaches 17.5 m, increasing pile length will cause material waste and increase construction cost. However, the failure probability of the slope is close to 1.4% when  $\delta_v=8$ m and pile length is 17.5 m, there is still a high risk of instability. According to Figs. 13 and 14, the average safety factor of the slope is greater than 1. From the perspective of safety factor, the slope is in a safety state, but the slope may still be destabilized and damaged.

Therefore, in the design of micro-pile, the influence of soil fluctuation range on the failure probability of the slope should be considered. Ignoring the influence of the fluctuation range may lead to the failure of the reinforced slope, resulting in casualties and economic losses. Increasing pile length can increase the mean of slope safety factor and reduce the failure probability of the slope, but excessive increase of pile length will increase construction difficulty and cost.

### 5.2 Influence of variation coefficient on structural reliability

As shown in Table 2, refer to previous research contents (Duncan 2000, Phoon 2008), the value range of  $COV_c$  is 0.19 ~ 0.55,  $COV_\phi$  is 0.05 ~ 0.4. The correlation coefficient between cohesion and friction angle is set to zero when investigating the effect of  $COV_c$  and  $COV_\phi$ . Therefore, set up seven groups from A to G to explore the influence of the variation coefficient, as shown in Table 3. In group A-D, the variation coefficient of cohesion decreases from 0.5 to 0.2,  $\delta_v=8$  m,  $\delta_h=40$  m. In group D-G, the variation coefficient of internal friction angle was increased from 0.05 to 0.2,  $\delta_v=8$  m,  $\delta_h=40$  m. Fig. 17 describes the mean and standard deviation of structural failure probability and slope safety factor corresponding to seven groups of different variation coefficients when pile length is 12.5 m and pile position is  $l_x/l=0.5$ .

As shown in Fig. 17, the variation coefficient has a small effect on the safety factor but a large effect on the probability of structural failure. With the increase of variation coefficient of strength parameters, the failure probability of slope shows an increasing trend. Although the average safety factor of the seven groups of data is greater than 1, the slope still has the risk of destabilization. Group D has the smallest variation coefficient, the spatial correlation of soil strength parameters is strong, which leads to weak variability of soil strength parameters. The failure probability of the slope is close to 11.6%. Group A has the largest variation coefficient of cohesion, Group G has the largest variation coefficient of internal friction angle, the spatial correlation of soil strength parameters is weaker, which leads to strong variability of soil strength parameters. The failure probability of slope is close to 34% and 42%.

The results show that the variation coefficient of a single strength parameter has a small effect on the slope safety factor. The effect on the slope safety factor can be ignored when the variation coefficient of soil strength parameters is small, but its effect on the probability of structural failure can't be ignored. The failure probability of the slope increases by nearly 31% when the variation coefficient of cohesion and internal friction angle increases from 0.2, 0.05 to 0.5, 0.2. Therefore, it is necessary to investigate the variation coefficient of soil strength parameters in the design of soil slope supported by micro-pile. Additional measures such as pile length should be taken to prevent slope instability when the variation coefficient of soil strength parameters is large.

## 6. Conclusions

In this work, based on the Latin Hypercube sampling method and K-L series expansion method, the cohesion and internal friction angle are taken as random variables to generate random field of strength parameters. The limit state equation of soil slope supported by micro-pile is obtained based on the limit equilibrium method. The effects of fluctuation range, variation coefficient on the reliability of soil slope supported by micro-pile are explored and the following conclusions are drawn:

- The micro-piles more effectively reinforce slopes when the pile position  $l_x/l$  is about 0.25. The reinforcement effect of micro-piles increases with the increase of pile length.
- The fluctuation range has a significant influence on the failure probability of soil slope supported by micro-pile. When the safety factor is greater than 1 and less than 1, the failure probability appears to be the opposite rule. The failure probability of the slope increases with the increase of fluctuation range when the mean safety factor of the slope is greater than 1. The failure probability of the slope increases by about 8.5% when the fluctuation range changes from  $\delta_v=2$  m to  $\delta_v=8$  m. The failure probability of the slope increases by about 2% when the fluctuation range changes from  $\delta_h=20$  m to  $\delta_h=60$  m.
- The variation coefficient has a significant influence on the failure probability of soil slope supported by micro-pile. The failure probability of the slope increases by nearly 31% when the variation coefficient of cohesion and internal friction angle increases from 0.2 and 0.05 to 0.5 and 0.2.

- The fluctuation range and variation coefficient have little influence on the mean value of safety factor. With the increase of fluctuation range, the safety factor shows an increasing trend. With the variation coefficient increasing, the safety factor shows a decrease trend.

## Acknowledgments

The research described in this paper was financially supported by Natural Science Foundation of Henan (232300421069); Central Plains Science and Technology Innovation Leader Project (234200510014); Program for Science and Technology Innovation Talents in Universities of Henan Province (24HASTIT014); Natural Science Foundation of Ningxia (2023AAC03036) and the First Class Discipline Construction in Ningxia (No. NXYLXK2021A03); Project of Science and Technology Department of Henan Provincial Department of Transportation (2022-5-5). These financial supports are gratefully acknowledged; Henan Provincial Key Laboratory of Grain and Oil Warehousing Construction and Safety Open Subjects (2020KF-B06).

## References

- Asaoka, A. and Agrivas, D. (1982), "Spatial variability of the undrained strength of clays", *J. Geotech. Eng. Division - ASCE*, **108**(5), 743-756. <https://doi.org/10.1061/AJGEB6.0001292>.
- Chen, F., Zhang, R., Wang, Y., Liu, H., Boehlke, T. and Zhang, W. (2020), "Probabilistic stability analyses of slope reinforced with piles in spatially variable soils", *Int. J. Approx. Reason.*, **122**, 66-79. <https://doi.org/10.1016/j.ijar.2020.04.006>.
- Cheng, H., Chen, J., Chen, R., Chen, G. and Zhong, Y. (2018), "Risk assessment of slope failure considering the variability in soil properties", *Comput. Geotech.*, **103**, 61-72. <https://doi.org/10.1016/j.compgeo.2018.07.006>.
- Chiasson, P., Lafleur, J., Soulie, M. and Law, K.T. (1995), "Characterizing spatial variability of a clay by geostatistics". *Can. Geotech. J.*, **32**(1), 1-10. <https://doi.org/10.1139/t95-001>.
- Cho, S.E. (2010), "Probabilistic assessment of slope stability that considers the spatial variability of soil properties", *J. Geotech. Geoenviron. Eng.*, **136**(7), 975-984. [https://doi.org/10.1061/\(asce\)gt.1943-5606.0000309](https://doi.org/10.1061/(asce)gt.1943-5606.0000309).
- Degroot, D.J. and Baecher, G.B. (1993), "Estimating autocovariance of insitu soil properties", *J. Geotech. Eng. - ASCE*, **119**(1), 147-166. [https://doi.org/10.1061/\(asce\)0733-9410\(1993\)119:1\(147\)](https://doi.org/10.1061/(asce)0733-9410(1993)119:1(147)).
- Deng, D., Li, L. and Zhao, L. (2017), "Limit-equilibrium method for reinforced slope stability and optimum design of antislides micro-pile parameters", *Int. J. Geomech.*, **17**(2). [https://doi.org/10.1061/\(asce\)gm.1943-5622.0000722](https://doi.org/10.1061/(asce)gm.1943-5622.0000722).
- Duncan, J.M. (2000), "Factors of safety and reliability in geotechnical engineering", *J. Geotech. Geoenviron. Eng.*, **126**(4), 307-316. [https://doi.org/10.1061/\(asce\)1090-0241\(2000\)126:4\(307\)](https://doi.org/10.1061/(asce)1090-0241(2000)126:4(307)).
- Fenton, G.A. and Griffiths, D.V. (2003), "Bearing-capacity prediction of spatially random c-phi soils", *Can. Geotechn. J.*, **40**(1), 54-65. <https://doi.org/10.1139/t02-086>.
- Fenton, G.A. and Vanmarcke, E.H. (1991), "Spatial variation in liquefaction risk assessment", *Geotech. Eng. Congress ASCE*, 594-607. <https://doi.org/10.1680/geot.1998.48.6.819>.
- Griffiths, D.V. and Fenton, G.A. (2004), "Probabilistic slope stability analysis by finite elements", *J. Geotech. Geoenviron.*

- Eng.*, **130**(5), 507-518. [https://doi.org/10.1061/\(asce\)1090-0241\(2004\)130:5\(507\)](https://doi.org/10.1061/(asce)1090-0241(2004)130:5(507)).
- Griffiths, D.V., Huang, J. and Fenton, G.A. (2009), "Influence of spatial variability on slope reliability using 2-d random fields", *J. Geotech. Geoenviron. Eng.*, **135**(10), 1367-1378. [https://doi.org/10.1061/\(asce\)gt.1943-5606.0000099](https://doi.org/10.1061/(asce)gt.1943-5606.0000099).
- Griffiths, D.V., Huang, J. and Fenton, G.A. (2011), "Probabilistic infinite slope analysis", *Comput. Geotech.*, **38**(4), 577-584. <https://doi.org/10.1016/j.compgeo.2011.03.006>.
- Huang, D., Song, Y., Ma, G., Pei, X. and Huang, R. (2019), "Numerical modeling of the 2008 Wenchuan earthquake-triggered Niuniangou landslide considering effects of pore-water pressure", *Bull. Eng. Geol. Environ.*, **78**(7), 4713-4729. <https://doi.org/10.1007/s10064-018-01433-7>.
- Javankhoshdel, S., Luo, N. and Bathurst, R.J. (2017), "Probabilistic analysis of simple slopes with cohesive soil strength using RLEM and RFEM", *Georisk-Assessment and Management of Risk for Engineered Systems and Geohazards*, **11**(3), 231-246. <https://doi.org/10.1080/17499518.2016.1235712>.
- Jiang, S., Li, D., Cao, Z., Zhou, C. and Phoon, K. (2015), "Efficient system reliability analysis of slope stability in spatially variable soils using monte carlo simulation", *J. Geotech. Geoenviron. Eng.*, **141**(2). [https://doi.org/10.1061/\(asce\)gt.1943-5606.0001227](https://doi.org/10.1061/(asce)gt.1943-5606.0001227).
- Li, C., Lin, M. and Huang, W. (2019), "Interaction between pile groups and thrust faults in a physical sandbox and numerical analysis", *Eng. Geol.*, **252**, 65-77. <https://doi.org/10.1016/j.enggeo.2019.02.023>.
- Li, X., Zhang, L., Gao, L. and Zhu, H. (2017), "Simplified slope reliability analysis considering spatial soil variability". *Eng. Geol.*, **216**, 90-97. <https://doi.org/10.1016/j.enggeo.2016.11.013>.
- Liu, X., Li, D.Q., Cao, Z.J. and Wang, Y. (2019), "Adaptive Monte Carlo simulation method for system reliability analysis of slope stability based on limit equilibrium methods", *Eng. Geol.*, **264**, 105384. <https://doi.org/10.1016/j.enggeo.2019.105384>.
- Luo, N., Bathurst, R.J. and Javankhoshdel, S. (2016), "Probabilistic stability analysis of simple reinforced slopes by finite element method", *Comput. Geotech.*, **77**, 45-55. <https://doi.org/10.1016/j.compgeo.2016.04.001>.
- Luo, Z. and Hu, B. (2019), "Probabilistic design model for energy piles considering soil spatial variability", *Comput. Geotech.*, **108**, 308-318. <https://doi.org/10.1016/j.compgeo.2019.01.003>.
- Mao, W., Liu, B., Rasouli, R., Aoyama, S. and Towhata, I. (2019), "Performance of piles with different configurations subjected to slope deformation induced by seismic liquefaction", *Eng. Geol.*, **263**, 105355. <https://doi.org/10.1016/j.enggeo.2019.105355>.
- Mayer, J.M. and Stead, D. (2017), "A comparison of traditional, step-path, and geostatistical techniques in the stability analysis of a large open pit", *Rock Mech. Rock Eng.*, **50**(4), 927-949. <https://doi.org/10.1007/s00603-016-1148-0>.
- Pang, R., Xu, B., Zhou, Y. and Song, L. (2021), "Seismic time-history response and system reliability analysis of slopes considering uncertainty of multi-parameters and earthquake excitations", *Comput. Geotech.*, **136**, 104245. <https://doi.org/10.1016/j.compgeo.2021.104245>.
- Pang, R., Zhou, Y., Chen, G., Jing, M. and Yang, D. (2023), "Stochastic mainshock-aftershock simulation and its applications in dynamic reliability of structural systems via DPIM", *J. Eng. Mech.*, **149**(1), 04022096. [https://doi.org/10.1061/\(ASCE\)EM.1943-7889.0002176](https://doi.org/10.1061/(ASCE)EM.1943-7889.0002176).
- Phoon, K.K. (2008), "Reliability-based design in geotechnical engineering: Computations and applications", Taylor and Francis, New York, NY, USA.
- Phoon, K.K. and Kulhawy, F.H. (1999a), "Characterization of geotechnical variability", *Can. Geotech. J.*, **36**(4), 612-624. <https://doi.org/10.1139/t99-038>.
- Phoon, K.K. and Kulhawy, F.H. (1999b), "Evaluation of geotechnical property variability", *Can. Geotech. J.*, **36**(4), 625-639. <https://doi.org/10.1139/cgj-36-4-625>.
- Soulie, M., Montes, P. and Silvestri, V. (1990), "Modeling spatial variability of soil parameters", *Can. Geotech. J.*, **27**(5), 617-630. <https://doi.org/10.1139/t90-076>.
- Suchomel, R. and Masin, D. (2010), "Comparison of different probabilistic methods for predicting stability of a slope in spatially variable c-phi soil", *Comput. Geotech.*, **37**(1-2), 132-140. <https://doi.org/10.1016/j.compgeo.2009.08.005>.
- Tang, L., Cong, S., Xing, W., Ling, X., Geng, L., Nie, Z. and Gan, F. (2018), "Finite element analysis of lateral earth pressure on sheet pile walls", *Eng. Geol.*, **244**, 146-158. <https://doi.org/10.1016/j.enggeo.2018.07.030>.
- Teixeira, A., Honjo, Y., Correia, A.G. and Henriques, A.A. (2012), "Sensitivity analysis of vertically loaded pile reliability", *Soils Found.*, **52**(6), 1118-1129. <https://doi.org/10.1016/j.sandf.2012.11.025>.
- Wan, Y., Fu, H. and Wang, Y. (2023), "Study on the influence of spatial variability of soil strength parameters on reliability and slip surfaces of cofferdam slope reinforced by geosynthetic reinforcement", *Mar. Georesour. Geotech.*, **42**(3), 233-242. <https://doi.org/10.1080/1064119X.2023.2169650>.
- Wang, Y., Han, M., Li, B. and Wan, Y. (2022b), "Stability evaluation of earth-rock dam reinforcement with new permeable polymer based on reliability method", *Constr. Build. Mater.*, **320**, 126294. <https://doi.org/10.1016/j.conbuildmat.2021.126294>.
- Wang, Y., Fu, H., Wan, Y. and Yu, X. (2022a), "Reliability and parameter sensitivity analysis on geosynthetic-reinforced slope with considering spatial variability of soil properties", *Constr. Build. Mater.*, **350**, 128806. <https://doi.org/10.1016/j.conbuildmat.2022.128806>.
- Wang, Y., Shao, L., Wan, Y. and Chen, H. (2024), "Reliability analysis of three-dimensional reinforced slope considering the spatial variability in soil parameters", *Stochastic Environ. Res. Risk Assessment*, 1-14. <https://doi.org/10.1007/s00477-023-02636-5>.
- Wang, Y., Shao, L., Wan, Y., Jiang, R. and Yu, X. (2023), "Three-dimensional reliability stability analysis of earth-rock dam slopes reinforced with permeable polymer", *Probabilist. Eng. Mech.*, **74**, 103537. <https://doi.org/10.1016/j.probengech.2023.103537>.
- Xu, B., Pang, R. and Zhou, Y. (2020), "Verification of stochastic seismic analysis method and seismic performance evaluation based on multi-indices for high CFRDs", *Eng. Geol.*, **264**. <https://doi.org/10.1016/j.enggeo.2019.105412>.
- Zhang, F., Ge, B., Leshchinsky, D., Shu, S. and Gao, Y. (2023), "Effects of multitered configuration on the internal stability of GRS walls", *J. Geotech. Geoenviron. Eng.*, **149**(12), 04023122. <https://doi.org/10.1061/JGGEFK.GTENG-11723>.
- Zhang, W., Wang, Q., Chen, F., Chen, L., Wang, L., Wang, L., Zhang, Y., Wang, Y. and Zhu, X. (2021), "Reliability analysis of slope and random response of anti-sliding pile considering spatial variability of rock mass properties", *Rock Soil Mech.*, **42**(11), 3157-3168. <https://doi.org/10.16285/j.rsm.2021.0464>.
- Zhou, G., Esaki, T., Mitani, Y., Xie, M. and Mori, J. (2003), "Spatial probabilistic modeling of slope failure using an integrated GIS Monte Carlo simulation approach", *Eng. Geol.*, **68**(3-4), 373-386. [https://doi.org/10.1016/s0013-7952\(02\)00241-7](https://doi.org/10.1016/s0013-7952(02)00241-7).